Integration of Microlens with Planar Lightwave Circuit

Author/Contributor:
Mackenzie, Mark; Kwok, Chee; Peng, Gang-Ding

Publication details:
Photonics West 2005
pp. 30-38

Event details:
Photonics West 2005
San Jose, USA

Publication Date:
2005

Publisher DOI:
http://dx.doi.org/10.1117/12.591373

Integration of microlens with planar lightwave circuit

Mark Mackenzie, Chee Yee Kwok and G. D. Peng
The University of New South Wales

ABSTRACT

A silica micro-lens pair has been proposed which can be integrated with planar optical waveguide circuits. The lens pair enables an optical signal to travel in free space between two opposing planar waveguides with minimal optical loss. Each lens in the lens pair consists of a slab GRIN lens with a convexly shaped front face. This paper briefly reviews the micro-lens design process and reports progress in fabricating the device. The characterisation of the GRIN layer and masking experiments used to evaluate the deep oxide etch are presented. A selectivity of 250:1 was achieved for the deep oxide etch using a NiCr mask.

Keywords: Silica, RIE, Microlens, Graded index

1. INTRODUCTION

A silica microlens pair has been proposed[1] for use in planar optical waveguide circuits. The lens consists of germanium doped silica with a parabolically graded refractive index profile (essentially a slab GRIN lens) to focus light in the vertical direction and a curved front-face to focus light in the horizontal direction.

The integrated waveguide lens pair is illustrated in Fig. 1. The lens pair allows free-space propagation of an optical signal between two opposing waveguides with minimal loss.

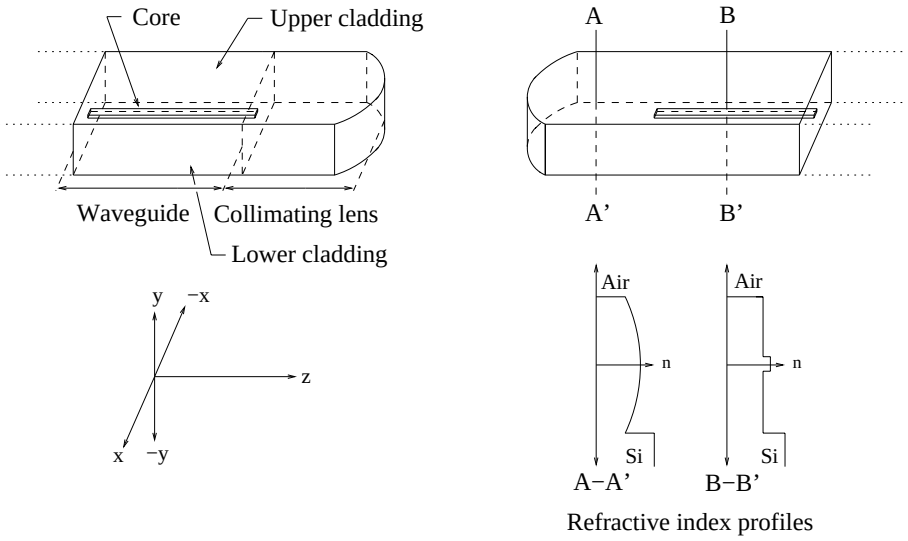

Figure 1. Integrated collimating waveguide lens pair.

The lens pair has potential application in optical interconnects, micro-optical switching and optical sensing. In this paper, the process for designing the micro-lens pair is reviewed, and progress in fabricating the lens pair is presented. The slab GRIN lens is characterised and a series of etching experiments were undertaken to determine the most suitable etch mask and conditions.

Further author information:
Mark R. Mackenzie: E-mail: markm@unsw.edu.au, Telephone: 612 9385 5395
Chee Yee Kwok: E-mail: c.kwok@unsw.edu.au, Telephone: 612 9385 5300
G. D. Peng: E-mail: g.peng@unsw.edu.au, Telephone: 612 9385 4014
Address: School of EE&T, The University of New South Wales, Sydney 2052, Australia

Photonics Packaging and Integration V, edited by Randy A. Heyler, Ray T. Chen,
Proceedings of SPIE Vol. 5731 (SPIE, Bellingham, WA, 2005)
0277-786X/05/$15 · doi: 10.1117/12.591373

2. LENS PAIR DESIGN

The lens pair design is based on the propagation of a scalar Gaussian field in materials of both constant and parabolically varying refractive index. Within the waveguide lens, the beam will have an elliptic shape in the cross-sectional plane but this 'elliptic' Gaussian beam can be considered as two independently propagating 'circular' Gaussian beams.[2]

Fig. 2 and Fig. 3 show the evolution of the vertical and horizontal spot-sizes as the optical beam propagates through the lens pair and the free space region. To achieve minimal propagation loss, the Gaussian parameters of the optical beam are matched at the point where it leaves the guided section of the transmitting lens (A-A' in Fig. 2 and Fig. 3), to the point where it enters the waveguide of the receiving lens (B-B' in Fig. 2 and Fig. 3). Because the receiving lens is a mirror image of the transmitting lens, this matching condition implies that the propagating Gaussian beam should be symmetrical about the centre of the free space propagation distance. Fig. 2 and Fig. 3 illustrate this symmetry.

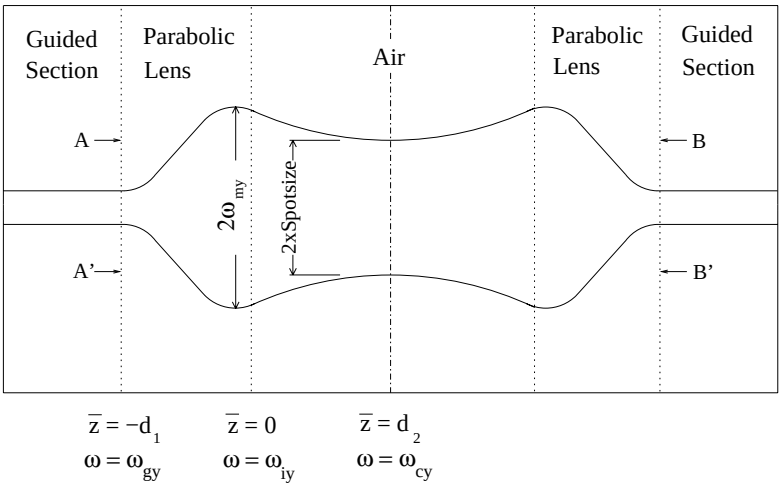

Figure 2. Evolution of vertical spot-size ω_y with propagation

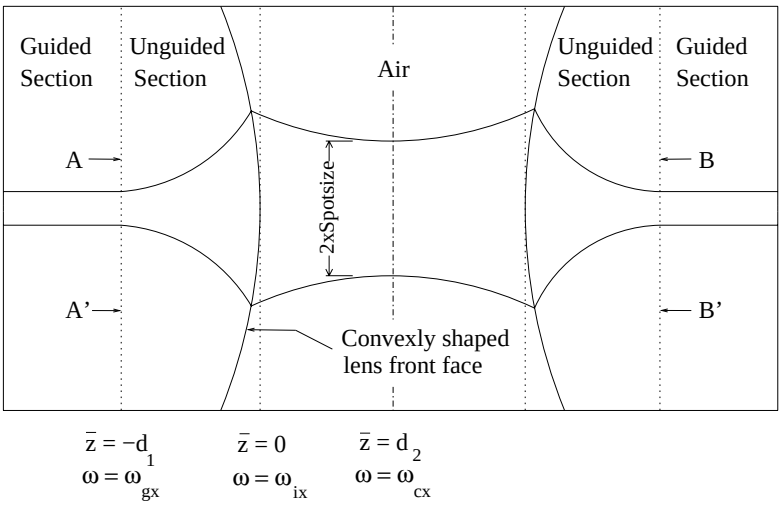

Figure 3. Evolution of horizontal spot-size ω_x with propagation

The formulae used to determine the parameters of the Gaussian beam in the two propagating media (parabolic graded index profile and constant refractive index) can be found in any standard text.[2] The resulting micro-lens design used to achieve a free space propagation of $200\mu m$ is presented in table 1 (see Ref 1. for further details).

Parameter	Description*
$d_2 = 100\mu m$	Half of free-space propagation length†
$\omega_{cy} = 9.3\mu m$	Minimum free-space vertical spot-size†
$\omega_{iy} = 10.7\mu m$	Interface vertical spot-size‡
$\omega_{my} = 11.0\mu m$	Maximum vertical spot-size in lens‡
$\omega_{gy} = 4\mu m$	Waveguide vertical spot-size†
$d_1 = 236\mu m$	Lens length‡
$n_o = 1.4545$	Maximum index of parabolic gradient†
$n_2 = 8.6 \times 10^{-5}$	Second order term of parabolic gradient‡
$\omega_{gx} = 4\mu m$	Waveguide horizontal spot-size†
$\omega_{ix} = 20.4\mu m$	Interface horizontal spot-size‡
$\omega_{cx} = 20.3\mu m$	Minimum free-space horizontal spot-size‡

Table 1. Interdependent waveguide parameters

*For the purposes of designing the minimal loss lens pair, the values of parameters marked † will be considered primary design parameters. The parameters marked ‡ are dependent on these primary design parameters.

3. PROPOSED FABRICATION STRATEGY

The lens pair can fabricated using a series of silica deposition and etching steps. Silica layers are deposited using the well known *Plasma Enhanced Chemical Vapour Deposition* (PECVD) process, and etched using *Reactive Ion Etching* (RIE) techniques.

1. PECVD lower cladding $n_2 = 1.4575$, $10\mu m$ thick.
2. Sputter 1000Å Cr for alignment marks.
3. Pattern Cr alignment marks.
4. PECVD core $n_1 = 1.4545$, $5 \pm .2um$ thick. $n_1 - n_2 = 0.007 \pm 0.001$
5. Pattern core, $3.5\mu m$ resist.
6. RIE core (Fig. 4a).
7. PECVD upper cladding $n_2 = 1.4575$, $6 \rightarrow 7\mu m$ thick (Fig. 4b).
8. Deposit silica RIE masking material.
9. Pattern masking material with square waveguide end-faces.
10. RIE to substrate surface, $21 \rightarrow 22\mu m$ (Fig. 4c).
11. PECVD silica with parabolically graded refractive index $\approx 25\mu m$ thick (Fig. 4d).
12. Planarise – remove $25\mu m$ (Fig. 4e).
13. Deposit silica RIE masking material.
14. Pattern masking material with curved front face.
15. RIE to Si surface $\approx 25\mu m$ (Fig. 4f).

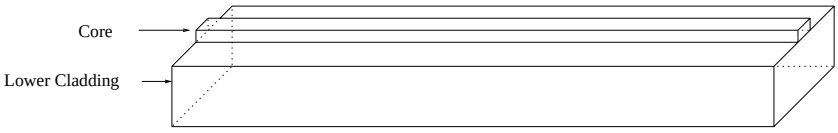

Figure 4a. After deposition of lower cladding and core, and RIE of core.

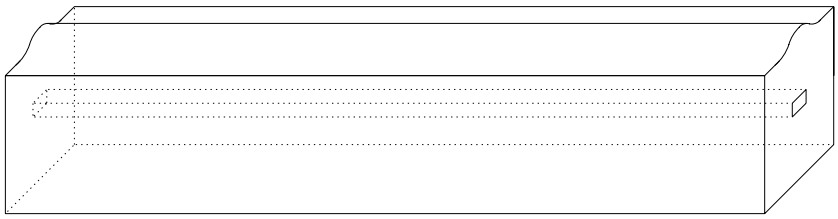

Figure 4b. After depositing upper cladding.

Figure 4c. After RIE to substrate surface.

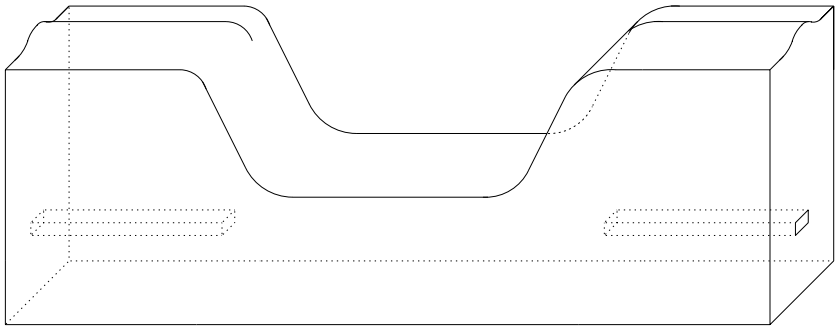

Figure 4d. After PECVD GRIN layer.

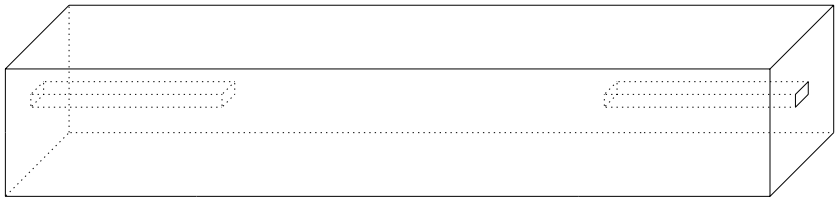

Figure 4e. After planarisation.

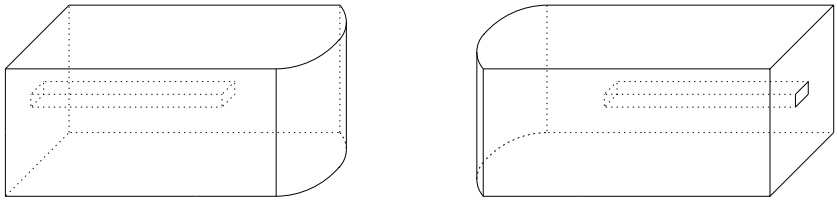

Figure 4f. After curved front-face etch.

4. EXPERIMENTAL

4.1. PECVD silica GRIN layer

A *Hollow Cathode*-PECVD reactor[3] has been used for the silica deposition. An RF plasma is developed in a silane (SiH_4) and oxygen mixture which causes silica (SiO_2) to form and adhere to the silicon substrate placed in the plasma chamber.

The refractive index of the silica is varied by adding germane (GeH_4) to the silane precursor gas mixture. This causes germanium to be incorporated into the silica matrix, increasing the refractive index of the film. The refractive index of the deposited silica films depends on a number of factors such as reactor configuration, RF power and chamber pressure.[3] A calibration procedure must be undertaken for each set of processing conditions.

Fig. 5 and Fig. 6 show the refractive index and thickness variation as a function of germane flow rate for a silane flow rate of 50 sccm. The refractive index and thickness of the films was measured using the prism coupler method which has an accuracy of ± 0.0005.[4] Using our reactor configuration and processing conditions the run to run variation in refractive index was less than 0.002. The variation in film thickness was approximately 3%. Work is currently underway to improve film uniformity and process variability.

In order to verify the graded refractive index layer is periodically refocusing the propagating light as expected, a polymer with a fluorescent dye[5] was spun onto a specially fabricated GRIN layer.

The GRIN layer was fabricated with the profile described by equation (1), using the parameters given in table 2.

$$n^2 = n_o^2 \left[1 - 2\Delta \left(\frac{y}{\rho} \right)^2 \right] \tag{1}$$

The polymer PVP was doped with Phloxine B using the procedure outlined in Ref. 5. A frequency doubled Nd:Yag laser (green) was launched into the GRIN layer via a fibre. As the laser light is refocused by the GRIN

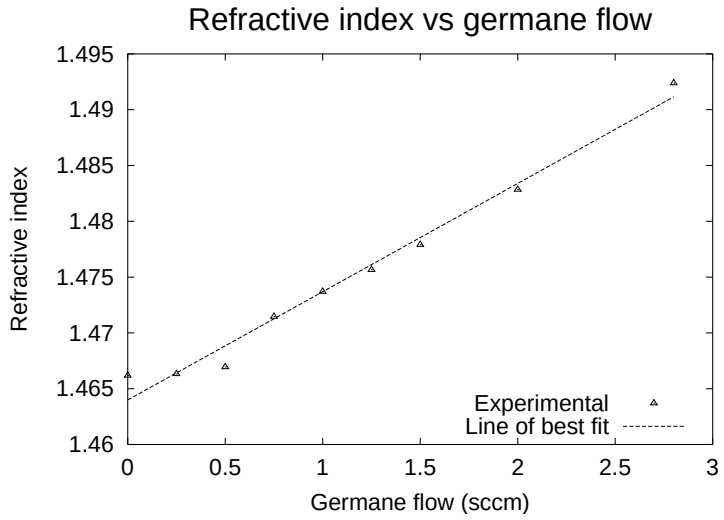

Figure 5. Refractive index of PECVD silica film as a function of germane flow. Chamber pressure = 15mTorr, RF power = 400W, SiH_4 flow = 10 sccm, O_2 flow = 50 sccm, Deposition time = 20 min.

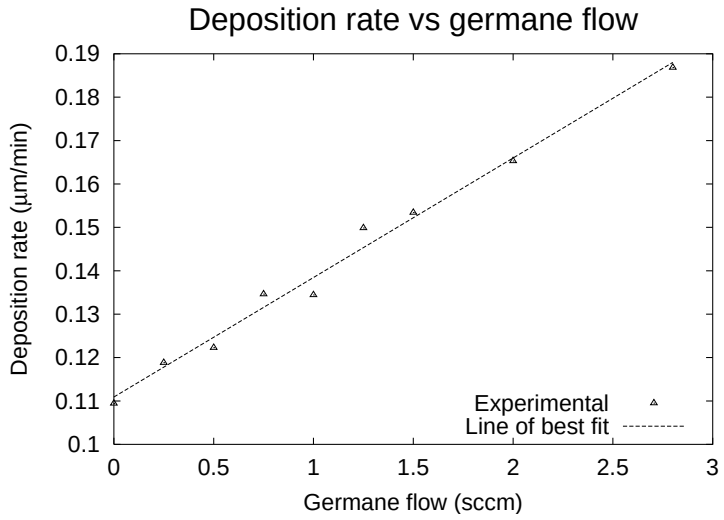

Figure 6. Deposition rate of PECVD silica film as a function of germane flow. Chamber pressure = 15mTorr, RF power = 400W, SiH_4 flow = 10 sccm, O_2 flow = 50 sccm, Deposition time = 20 min.

Parameter	Value	Description
n_o	1.49	Maximum refractive index (core)
ρ	$18.8\mu m$	Half-width of parabolic profile
Δ	0.01	Refractive index difference at half-width ρ
n_{step}	0.001	Refractive index step size

Table 2. Fabricated GRIN layer parameters.

layer, the phloxine dye fluoresces with a yellow colour. A photograph is shown in Fig. 7. Ten of the fringe spacings occur within a spacing of 3.5mm, leading to a refocus length $z_{\text{refocus}} = 350\mu m$.

This demonstrates that the periodic focusing of the GRIN lens does indeed work.

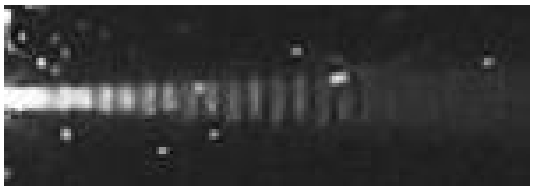

Figure 7. Periodic refocusing of GRIN layer. The pattern has a period of $350\mu m$.

4.2. Deep silica RIE

The etching of the lens convex curvature is by no means a trivial matter. The process has stringent requirements on sidewall verticality and surface roughness, and is of considerable depth.

Reactive ion etching (RIE) is the preferred etching method because it allows an anisotropic profile to be obtained. RIE has been used in the semiconductor industry over the last few decades, however semiconductor fabrication generally only requires etch depths of less than $1\mu m$. Fabrication of the lens pair requires etches to a depth of $30\mu m$ or more.

The RIE of the silica is the most difficult part of the fabrication process to be carried out at the University of NSW due to the limited RIE fabrication facilities available. In a typical production environment, the deep silica etch could be achieved using an inductively coupled plasma (ICP) RIE machine such as the *STS Advanced Oxide Etch* and a thick polysilicon masking material.[6]

For the purposes of validating the microlens design (in the absense of advanced oxide etch equipment), a variety of masking materials and plasma etch conditions were trialled to obtain optimum etch conditions at the expense overall etch rate. The results presented in Table 3 were performed using a Hollow-Cathode RIE (HC-RIE) reactor.[3] The HC-RIE is essentially a parallel plate reactor with two opposing electrodes which are both driven by the same RF source.

Electroplated nickel[7] has been used for deep oxide etches with a selectivity of approximately 20:1. However we found that electroplated nickel had a relatively low sputter threshold and grass problems were difficult to eliminate.

Mask	Power (W)	Pressure (Pa)	CF_4 (sccm)	SF_6 (sccm)	O_2 (sccm)	Selectivity	V_{dc}
Cr	200	30	15		3	35:1	
Cr	200	15		15	3	32:1	-240
Cr	250	25		15	3	35:1	-164
Cr	200	1.5	15		3	30:1	-327
Cr	40	7.5	15		3	28:1	-120
Al	150	30	25		1.5	44:1	
Al	150	10		15	3	30:1	-166
Al	150	1.5	15			10:1	-324
NiCr	150	10		15	3	Etch slowed	-166
NiCr	200	15	10	15	3	100:1	-313
NiCr	125	10	10	10	4	160:1	-186
NiCr	150	30	25		1.5	Etch slowed	
NiCr	200	7.5	15		3	50:1	-370

Table 3. Mask and process conditions.

While the greatest selectivity was achieved using a NiCr mask, the etched silica surface became textured, the etch rate reduced and eventually etching ceases. This was found to be due to non-volatile etch reaction *products* – NiF_2 being sputtered and redepositing on the etched surface (as opposed the the etch mask material itself – NiCr). This also occurred when Al is used as an etch mask.

These results demonstrated a significant shortcoming of the HC-RIE. When material was sputtered from the etch surface it was deposited onto the opposing electrode. Since in the HC-RIE configuration the opposing electrode is also driven, it was then re-sputtered back to the etch surface. This caused the surface texturing problems which eventually caused etching to cease.

The hollow cathode reactor was modified by grounding the opposing electrode, effectively converting the reactor to a standard parallel plate configuration albeit with a narrow electrode spacing. This produced a relatively intense plasma from just 32W forward RF power. CF_4 and O_2 were used at 7.5 Pa with a 1500Å NiCr mask. Additionally, the etch sample was removed every hour and given an ultrasonic rinse in de-ionised water (DI). This was done to remove any buildup of nickel fluoride deposits.

Using this method a selectivity of $\approx 250:1$ was achieved. However, the etch-rate was only $1.2\mu m$ per hour, making this process unsuitable for a production environment.

The resulting etch is illustrated in Fig. 8. Beneath the silica lens the silicon substrate has been etched in TMAH to reduce coupling of light to the silicon.

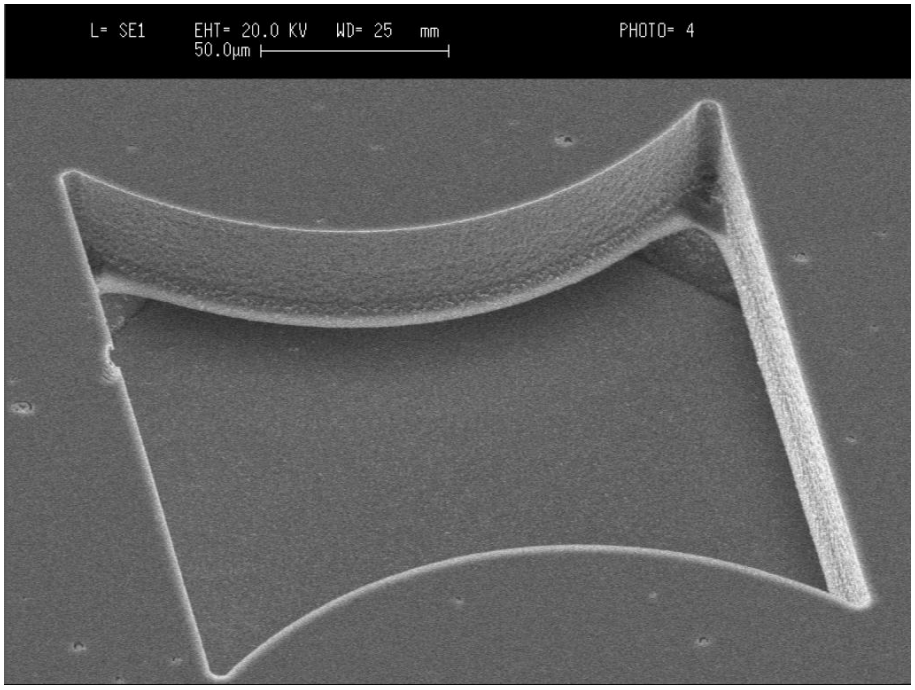

Figure 8. RIE of front face curvature.

5. CONCLUSION

An integrable silica microlens has been presented which has application in optical interconnects, micro-optical switches and optical sensing. The proposed fabrication strategy is detailed and progress in fabricating the device is shown. Optical characterisation of the device is underway and will be presented at the conference.

6. ACKNOWLEDGEMENT

The authors would like to thank the Australian Research Council for financial support in this research.

REFERENCES

1. M. R. Mackenzie and C. Y. Kwok, "Theoretical analysis of integrated collimating waveguide lens," *IEEE Journal of Lightwave Technology* **21**(4), pp. 1046–1052, 2003.
2. A. Yariv, *Optical Electronics*, CBS College Publishing, 1985.
3. M. V. Bazylenko, M. Gross, A. Simonian, and P. L. Chu, "Pure and flourine-doped silica films deposited in a hollow cathode reactor for integrated optic applications," *Journal of Vacuum Science Technology A* **14**(2), pp. 336–345, 1996.
4. Metricon, "Metricon model 2010 prism coupler application notes." www.metricon.com.
5. D. R. Beltrami, J. D. Love, A. Durandet, A. Samoc, and C. J. Cogswell, "Fabrication and characterization of a planar gradient-index, plasma-enhanced chemical vapor deposition lens," *Applied Optics* **36**(28), pp. 7143–7149, 1997.
6. J. K. Bhardwaj, C. Welch, A. Barker, R. Gunn, L. Lea, and S. Watcham, "Advances in deep oxide etch processing for mems - mask selection." www.stsystems.com.
7. X. Li, T. Abe, and M. Esashi, "Deep reactive ion etching of pyrex glass using sf_6 plasma," *Sensors and actuators A* **87**, pp. 139–145, 2001.